Real time digital pulse processing applied to heavy ion irradiation

Cristian Zet[1,2], Cristian Fosalau[1], Lars Westerberg[3], and Reimar Spohr[2]

[1] *Technical University "G. Asachi" Iasi, Bd. D. Mangeron, 53, Iasi, 700050, Romania, phone +40 232 278683, fax +40 232 237627, czet@ee.tuiasi.ro, cfosalau@ee.tuiasi.ro*
[2] *Gesellschaft für Schwerionenforschung mbH, Planckstr. 1, 64291 Darmstadt, phone +49 6159 712725, fax +49 6159 712179, r.spohr@gsi.de, c.zet@gsi.de*
[3]*Lars Westerberg, Svedberg Laboratory, Uppsala University, Box 531, S-75121 Uppsala, Sweden, phone +46-18-471-3060, fax +46-18-471-3833, lars.westerberg@tsl.uu.se*

Abstract **-** Three algorithms for real-time digital pulse processing of fast detector signals (1-100µs) are described and implemented through Field Programmable Gate Arrays (FPGAs). The signal from a PIN diode used as ion detector is amplified and digitized with a fast flash ADC at a rate of 10 MHz/s. Whenever a preset threshold is exceeded, an event is detected. The pulse maximum is determined using one of the three methods, characterized by decreasing response times and increasing the result confidence degree: (1) searching for the maximum, (2) integrating the signal and (3) looking for the derivative sign. The system is applied to fabricate polymer films with a preset number of ion hits at preset distances. The technique can be generalized to real-time processing of pulsed signals from arbitrary sensors and transducers.

I. Introduction

Nuclear spectrometry is usually accomplished with analog processing electronics (amplifiers with analog pulse shaping and multi-channel analysers) to perform pulse-height analysis. Although capable of high count rates, this approach is not able to perform optimum signal-to-noise ratio pulse shaping and it is vulnerable to the physical imperfections of the electronic components. The random nature of pulse appearance in time due to the occurrence of the radiation, doubled by the imprecision of the detection process, leads to degradation of the measured spectrum [1]. This can be corrected by introducing supplementary processing blocks along the chain which, however, may introduce additional errors.

Digital and analog signal processing have certain similarities at conceptual level: extracting the information from the signal, suppressing the non-useful information, reducing the quantity of information to a manageable level, delivering data in an intelligible format [2]. For obtaining the best energy resolution, theoretical optimum filters should be used which can be implemented only by digital methods [3].

II. Pulse processing in heavy ion irradiation experiments

Since the early 50s pulse spectrometry has been playing an important role in many fields: medicine, industry, science. Its home base is nuclear physics, where pulsed signal sources are common and large numbers of events have to be analyzed, including their statistical properties.

The main function of a pulse analyzer is to record and display their amplitude distribution function of the ion pulses [4]. A Multi-Channel Analyzer (MCA) is a dedicated instrument for this task. It divides the amplitude range in a number of equally spaced intervals or bins, so called channels. Each channel holds the number of events in the corresponding range of amplitudes. Each pulse leads to one unit increment of the channel to which is attributed. The number of channels the system is capable to distinguish defines the systems energy resolution.

Early instruments were based on electromechanical sorters. They converted the amplitude into a mechanical impulse that would eject a ball with a velocity proportional to the amplitude [4]. Later, MCA's started to incorporate integrated circuits, and to shrink their volume. The microprocessor enabled to increase the processing speed and the data volume. About a decade ago, fast ADCs combined with VLSI digital circuits completely changed the face of pulse processing. The conventional analog front end has been replaced by a digital pulse processor that computes the pulse-height from the data sampled by the fast ADC. This approach allows avoiding non-linearities and instabilities of the analog front-end plus the flexibility offered by the programmable nature of the

digital circuitry. Although the most versatile way to implement a digital pulse processor is through software, the large computation time required prohibits real-time analysis and thus limits its practical use. In particular, at high throughput rates, hardware digital pulse processing must be used. This solution is reducing from the versatility when compared with the software but development time and speed are superior. The electronic development nowadays enables very fast digital signal processing at high clock frequencies.

II. Polymer film irradiation system – application for pulse processing

The purpose of the pulse processing system, described in detail below, is to be used into an irradiation system for polymer film with a preset number of ions in precisely marked positions along the tape's middle line with a reliability suited for a mass production (Figure 1). The system is placed at a heavy-ion accelerator. It allows the irradiation with a preset number of ions within a given target area and to automatically switch-off the beam after this is accomplished. The irradiation points can be placed at distances between millimetres and centimetres along the axis of the polymer film resulting in so-called film frames that can later-on be processed continuously or separately in batches down to one irradiation spot per sample.

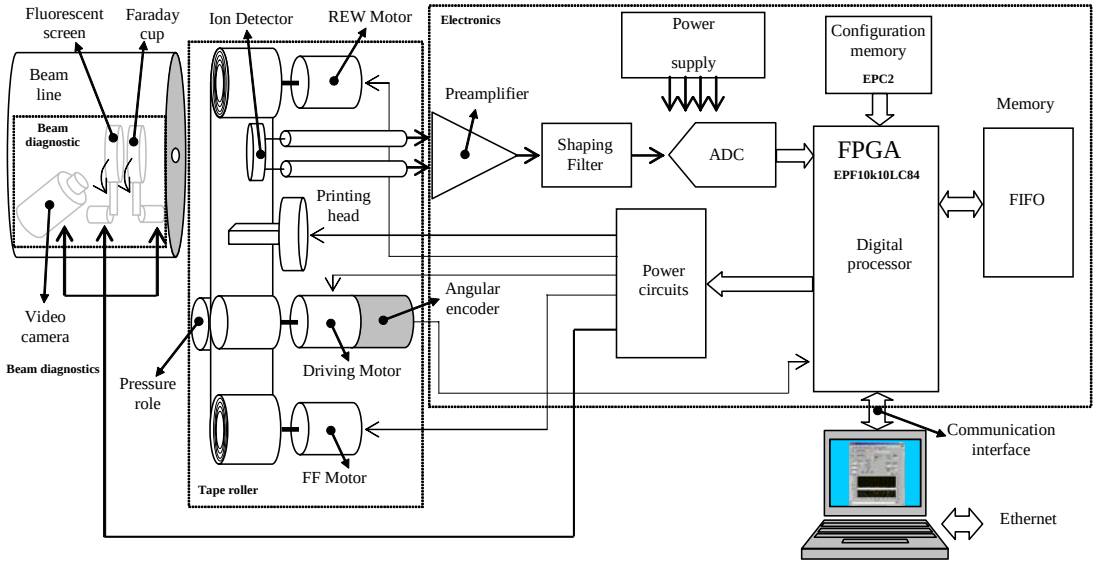

Figure 1. Block diagram of irradiation system

The main purpose of our pulse analysis system is to eliminate samples containing scattered ions, characterized by reduced energy. Since the fraction of scattered particles increases with the inverse of the aperture radius, the suppression of scattered particle becomes mandatory for apertures smaller than 10μm. As a beneficial side-effect of the performed pulse analysis the continuous monitoring of the detector efficiency becomes possible. Detector degradation is characterized by steadily decreasing pulse height. This effect, too, becomes important only for very high total counts deposited within a certain area of the ion detector. In our case, no apparent detector degradation was found for total pulse counts up to 10000 within a detector area of about 1 mm diameter (corresponding to a total fluence of about 10^6 ions/cm^2). We used as ion detector a so-called PIN-Detector (Hamamatsu silicon PIN diode [5]). In order to detect a possible degradation of the ion detector, or scattered particles with low energy, a pulse processing is necessary. Besides the digital pulse processor, the system includes an ion detector, placed as narrow as possible behind the polymer film, a preamplifier followed by a signal shaper and a fast ADC. Every ion, hitting the detector, produces a short pulse at the detector's terminals. The peak value of the pulse is proportional to the ion energy. The signal is amplified and shaped in order to minimize the influence of noise and pulse tail. The Real Time Digital Pulse Processor (RTDPP) is supplied with the data stream coming from the fast ADC. The RTDPP searches the peaks in the data stream, stores the values in a FIFO memory and deflects the beam when the desired number of ions has been detected

The peak height distribution is usually located in a narrow interval around a mean value. Due to scattering of the ions on the edge of the round aperture, the ion energy can fluctuate between zero energy and full ion energy. Scattered particles therefore can have different track etching rates. In

extreme cases, some of the scattered ions can get stuck and will not be recorded. Fortunately the corresponding ion tracks will usually end within the polymer film and thus not lead to perforations.

There exist several simple efficient algorithms suited for implementation in digital circuits. For example: (1) compare all samples data with a chosen threshold and look for the maximum value as long as the signal is above the threshold, (2) integrate the signal as long as the signal is above a chosen threshold and (3) use the signal's derivative. Due to the randomness of ion detection events, at high count rates multiple peaks can occur. This happens when two or more ions hit the detector with very short delays (delays which are smaller than the pulse tail). The second, third, etc pulses will be raised on the tails of the previous peaks, like in Figure 2. For very thick samples, the remaining ion energy can be too low to discriminate the ion pulses from the background noise.

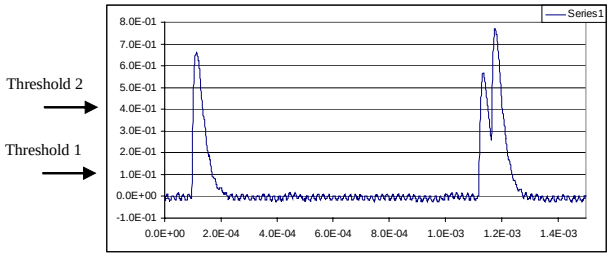

Figure 2. Single and multiple peaks

III. Architectures of digital peak detectors

The simplest algorithm (1) is to look for the maximum value within a defined time interval after exceeding the threshold. Each ADC sample is compared with the previous maximum detected value and replaces it if it is larger. This can be described by the following equation:

$$peak = \max_{k=0}^{N}\left(x_k\right); \quad \text{where} \begin{cases} x_0 \text{ is the first sample above the threshold} \\ x_N \text{ is the last sample above the threshold} \end{cases} \tag{1}$$

The process ends as soon as the signal has fallen below the threshold. A block diagram for such a peak detector is shown in Figure 3.

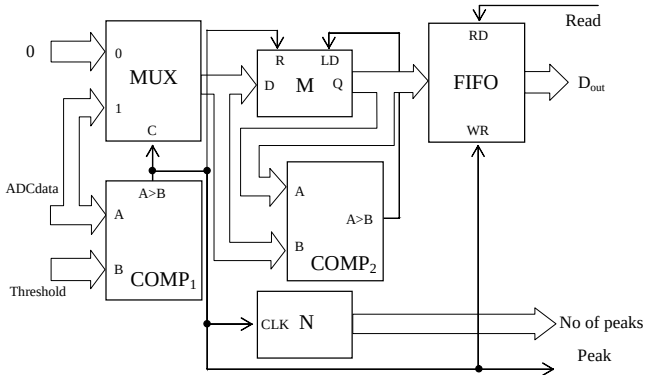

Figure 3. Peak detector – searching the maximum in a defined time interval

The implementation of this algorithm is very simple and works as follows. First, the data (D_{in}) are compared with the threshold (Threshold) by a digital comparator ($COMP_1$) to define the time interval. Using a multiplexer (MUX), only necessary samples are selected from the signal. The memory M and the digital comparator ($COMP_2$) perform the effective maximum searching. The memory is initialized with zero and at each clock the current sample is compared with the content in the memory. If the comparator detects a sample larger than the previous maximum, it replaces the old value in the memory M by activating the signal LD. The number of peaks is counted by the counter N and each peak value is stored in the FIFO memory. The memory M is cleared after the peak value is transferred into the FIFO memory. Figure 4 presents the waveforms associated for the peak detector.

ADCdata[7..0] represents the data coming from the ADC, and it is synchronous with the clock signal (clk). The data stream represents a real data stream generated by an ion hitting the detector ($Xe27^+$, 8.4MeV/nucleon). The maximum value is available immediately after it occurs, on the next rising edge

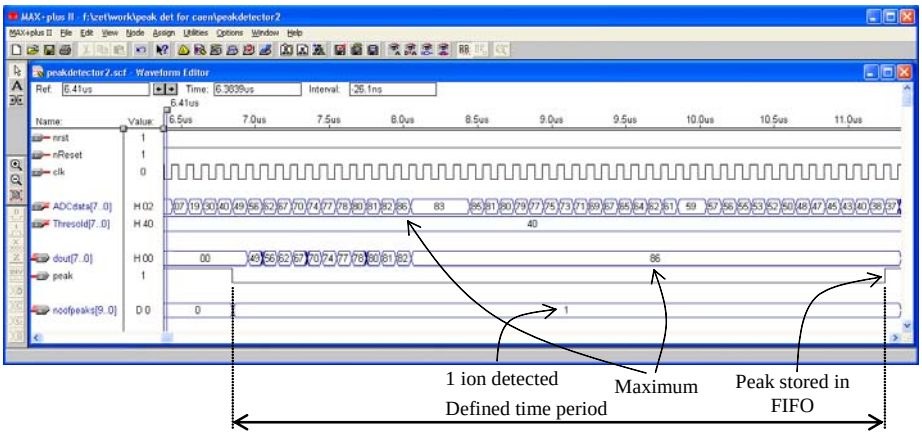

Figure 4. Waveforms associated to the peak detector (searching for maximum algorithm)

of the clock, but will be stored in memory at the end of the pulse.

For a reliable irradiation, it is necessary to detect every peak. Due to the fact that ion passage is a statistic event, they can occur at random moments in time. If the beam intensity is low enough, then the probability of such events is very low. The algorithm described above is not able to detect such close pulses (Figure 2), without using multiple thresholds and more complicated architecture.

Another algorithm that can be used is the one which integrates the signal during the pulse duration (2). This is suitable for weak signals buried in noise and/or in noisy environments, when the parasitic signal influence can be diminished by integration. It will also fail to detect close pulses. The digital hardware implementation of this algorithm is shown in Figure 5.

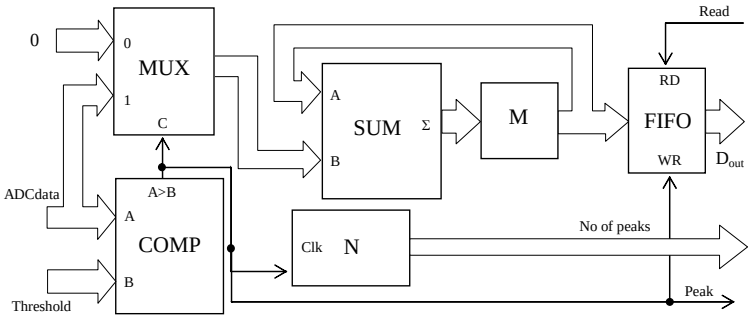

Figure 5 . Peak detector - signal integration

The surface restricted by the signal's curve and the time axis is proportional with the energy of the incident ion. This is helpful when the signal to noise ratio is low and the noise added to the signal is significant. Again is not necessary to compute the whole integral. Replacing it with a sum

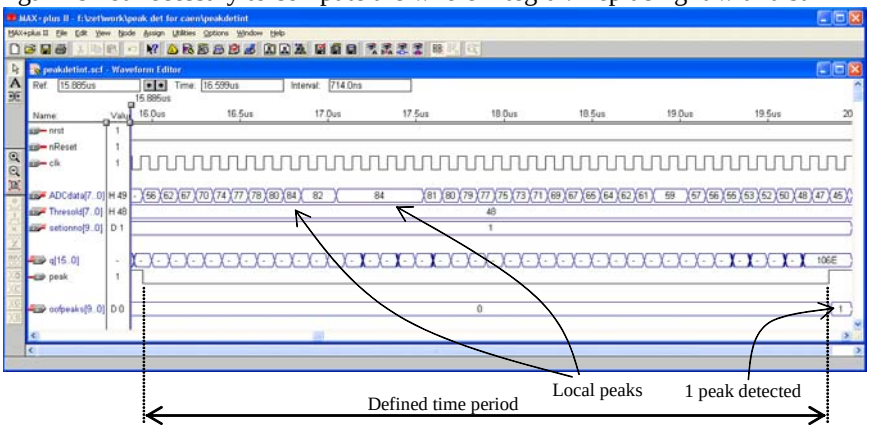

Figure 6 . Waveforms associated to the peak detector (integration algorithm)

$$E = \sum_{i=0}^{N} x_k \qquad (2)$$

simplifies the implementation. In the schematic above the ion detection part is identical but only the energy estimation is different. The digital comparator ($COMP_2$ in Figure 3) has been replaced with a summing block, the rest of the schematic remaining unchanged. The result has a larger number of bits, leading to a larger FIFO. The diagram can be improved by adding a dividing block in order to reduce the number of bits of the result. This will enlarge the area used on FPGA. The waveforms for this approach are presented in the Figure 6.

The third algorithm is using the first derivative as peak detection method. The derivative of the signal is changing the sign when the signal passes through a maximum or a minimum. Considering only the derivative change from positive to negative, only the peaks can be detected (Figure 7).

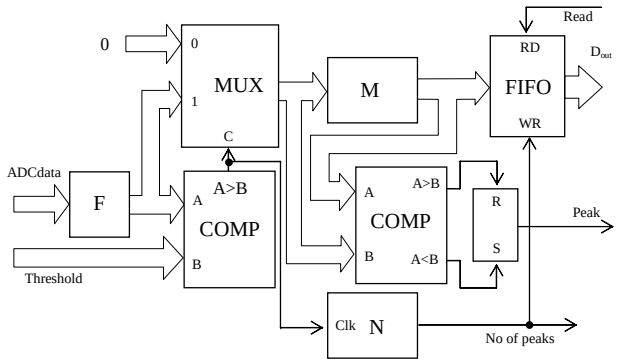

Figure 7. Peak detector - derivative algorithm

It is not necessary to compute the derivate values in every point

$$\frac{dx_k}{dt} = \frac{x_k - x_{k-1}}{T_S}, \text{ where } T_S \text{is the sampling period} \qquad (3)$$

because not the value is important, but the sign. This simplifies the implementation, because checking the sign is performed with a digital comparator.

The data stream is filtered first with a digital low pass filter (F), in order to smooth the signal. This is brings the benefit of integration and it is really necessary because the derivative will detect every local

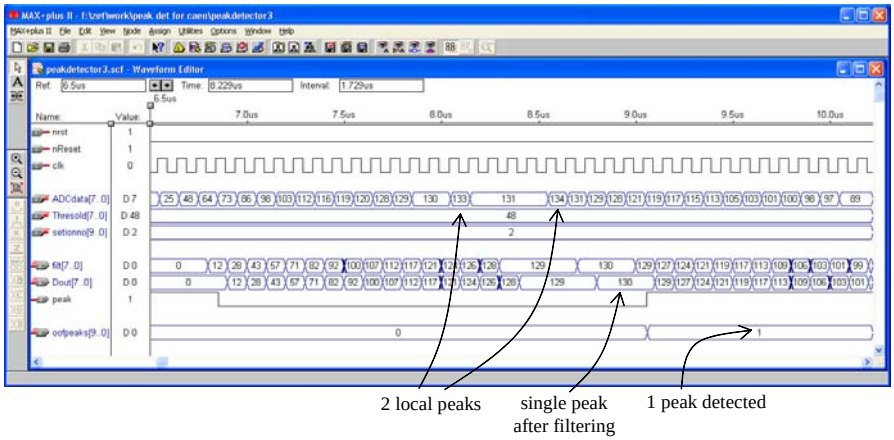

Figure 8. Waveforms associated to the peak detector (derivative algorithm)

peak in the signal. After separating the pulse from the rest of the signal (MUX), the derivative sign is checked (M and COMP). It is enough to compare consecutive samples in order to determine the sign of the derivative. Comparing with the previous algorithms, this one ends with the first sample after the peak (the response time is the pulse rise time). The waveforms associated are presented in Figure 8.

ADC data stream contains a pulse with two local peaks due to the noise added by the electronics. After filtering, the new data stream is smooth, presenting just a single peak. The positive edge of the signal “peak” stores the maximum value into the FIFO memory. For an appropriate PCB design, proper grounding and using a low noise amplifier, the signal is free of noise and the signal comes smooth even

before the filter F.

IV. Results and conclusions

Figure 9 shows the pulse height spectrum of a 8.3 MeV/u Xe 27^{+} ion beam, after penetrating a 25μm PET foil tilted by 35 degrees. The Gaussian pulse height distribution has mean value of 1.48V and a width of less than 1%. Very few scattered "bad" particles at lower energies than the average were recorded. Film frames corresponding to events inside the main peak were marked as "good" frames and all others were marked as "bad" frames.

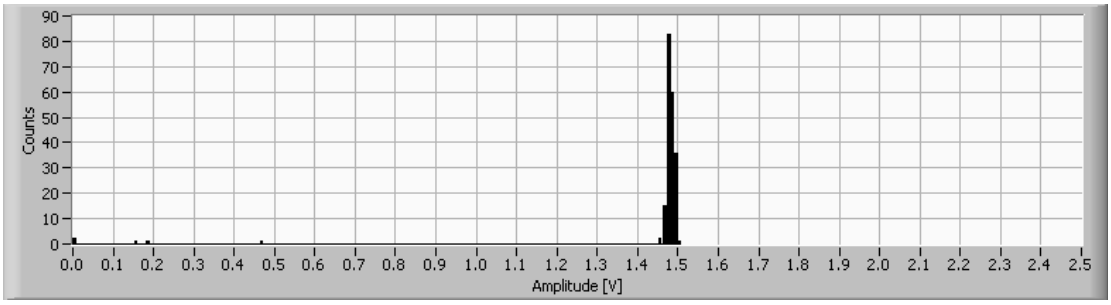

Figure 9. Energy distribution for Xe 27^{+} at 8.4MeV/μ through 25μm PET foil

Table 1 shows the area occupied by the three peak detectors (using Altera FPGA Flex10k10).

Table 1

	Looking for maximum	Integration	Derivative + LPF
Percentage of area	13%	13%	14%
Used logic cells	79	78	82

Table 2 compares the performances of the proposed peak detectors regarding detecting false local peaks, close peaks, confidence of the result and response time.

Table 2

	Looking for maximum	Integration	Derivative + LPF
Detect false peaks	NO	NO	NO
Detect close peaks	NO	NO	YES
Confidence	GOOD	GOOD	BEST
Response time	Pulse length (≅ 5μs)	Pulse length (≅ 5μs)	Pulse rise time (≅600ns)

Acknowledgement

This work was supported by the European Network on Ion Track Technology (Contract HPRN-CT-2000-00047).

References

[1] J.M.R. Cardoso, J. Basilio Simoes, C.M.B.A. Correia, “A mixed analog digital pulse spectrometer”, Nuclear Instruments and Methods in Physics research, A 422, pp. 400-404, 1999.

[2] W.K. Warburton, M. Momayezi, B. Hubbard Nelson, W. Skulski, “Digital Pulse processing: New possibilities in Nuclear Spectroscopy”, Conference on Industrial Radiation and Radioisotope Measurements and Applications IRRMA-99), Raleigh, NC, October 3-7, 1999.

[3] G. Bertuccio, A. Fazzi, A. Geraci, M. Sampietro, “An optimum digital signal processing for radiation spectroscopy”, Nuclear Instruments and Methods in Physics Research, A 353, pp. 257-260, 1994.

[4] J.B. Simoes, C.M.B.A- Correia, “Pulse processing architectures”, Nuclear Instruments and Methods in Physics Research, A 422, pp. 405-410, 1999.

[5] ****; “Si PIN photodiode S1223 series”, Hamamatsu Photonics K.K. – Solid-state division, Japan, Cat. No KSPD0001E01, Jan. 2002